学位論文（要約）

Ultrathin Gold Nanorods:
Controlled Synthesis and Characterization
(極細金ナノロッドの構造制御と物性評価)

平成29年12月博士 (理学) 申請

東京大学大学院理学系研究科

化学専攻

髙畑　遼

Abstract

Metal NSs have long attracted many researchers because of their unique properties, which are scalable by the diameter. For example, melting temperature is inversely proportional to the particle diameters. Another representative property is localized surface plasmon resonanes (LSPRs) that are collective oscillations of conduction electrons in response to incident light, intensifies with increase of the diameters. In contrast, metal clusters that are defined as further miniaturized NSs, exhibit novel properties, which are not scalable and predictable with the diameters. In case of gold, it is known that their structures and properties change drastically at a critical diameter of ~2 nm. The atomic structures of thiolate-protected Au clusters undergo a transition from fcc structure to icosahedral or decahedral structures when the diameter becomes smaller than 2 nm. The optical response of AuNSs also changes at this size region from LSPRs to single electron transition between quantized levels. Chemical properties of metal NSs also show non-scalabe behavior in the cluster regime. For instance, Au clusters exhibit catalytic activities for oxidation reactions.

We can regard anisotropy as another parameter to control the properties of metal nanostructures in addition to the diameters. The catalytic properties of Pt and Pd nanostructures depend strongly on their morphology. Gold nanorods (AuNRs) have been extensively studied as the representative anisotropic Au nanostructures. One of the attractive properties of AuNRs is LSPRs. AuNRs exhibit two LSPRs of transverse mode at around 500 nm and longitudinal mode in the vis–NIR region. The AuNRs are

expected to exhibit unique properties when their diameters become smaller than a critical size as observed in isotropic AuNSs. The synthesis of ultrathin gold nanowires (AuUNWs) with a diameter of ~1.6 nm and a length of μm scale has been reported. Fundamental questions arise as to how the structures, and basic properties of AuUNWs and ultrathin gold nanorods (AuUNRs) are different from those of conventional AuNRs. In order to answer these questions, we must overcome technical challenges that include controls of lengths while keeping the diameter of <2 nm, and observations of atomic structures of AuUNRs.

In Chapter 2, I reported synthetic methods of ultrathin gold nanorods (AuUNRs) by slow reductions of gold(I) in the presence of oleylamines (OAs) as surfactants. Transmission electron microscopy revealed that the lengths of AuUNRs were tuned in the range of 5−400 nm by changing the concentration of OA while keeping the diameter constant (~2 nm). The surfactant OA was successfully transformed into glutathionate or dodecanethiolate by ligand exchange approach.

In Chapter 3, I investigated the optical properties of AuUNWs and AuUNRs. AuUNRs exhibited a broad band in the IR region whose peak position was red-shifted with the length. Polarized extinction spectroscopy for the aligned AuUNWs indicated that the IR band was assigned to the longitudinal mode of LSPRs. Notably, the longitudinal LSPR wavelengths were significantly affected by the miniaturization of the diameter below ~2 nm: the longitudinal LSPR wavelengths for AuUNRs were remarkably longer than those of conventional AuNRs (diameter>10 nm) with the same

aspect ratio. The electromagnetic simulation suggested that the origin of the redshift was probably ascribed to the difference in permittivity.

In Chapter 4, in order to understand the structure−property correlation of AuUNRs, their atomic structures were examined using aberration-corrected high-resolution transmission electron microscopy. Statistical analysis revealed that the most abundant structure observed in AuUNRs was a multiply twinned crystal, with a periodicity of ~1.4 nm in length. I proposed that the AuUNRs were composed of cuboctahedral Au_{147} units, which were connected one-dimensionally through twin defects. The formation process of the atomic structures in AuUNRs that involved attachment of Au spherical clusters in OA micelles was proposed based on the time-resolved X-ray absorption spectroscopy and optical spectroscopy.

In Chapter 5, I studied the stability of AuUNRs and elucidated the decomposition process. I also found the method to improve the stability. AuUNR stabilized by OA were spheroidized when dispersed in chloroform containing a small amount of OA. Time-resolved optical spectroscopy and TEM analysis indicated that the AuUNRs were gradually shortened with the release of small Au nanospheres (AuNSs) because of Rayleigh instability, followed by transformation into plasmonic AuNSs (diameter >2 nm). The OA surfactants played an essential role in stabilizing the morphology of AuUNRs by suppressing the diffusion of Au surface atoms. The stability of AuUNRs was improved by the surface modifications by thiolate due to the suppression of surface diffusion of Au atoms.

In Chapter 6, I summarized this thesis and stated the future prospects as concluding remarks.

Contents

Chapter 1.

General introduction

1.1. Isotropic metal nanostructures

1.1.1. Metal nanospheres

Metal nanospheres (NSs) have long attracted many researchers because of their unique structural properties. Figure 1.1 shows a typical model of NSs with fcc morphology (cuboctahedron), which are constructed by truncation of cubic fcc nanocrystals. Unique properties will be emerged due to the nano-size effects. In this section, a brief overview how the structures and properties of isotropic metal NSs change with the diameters.

The most prominent structural feature of metal NSs is that the fraction exposed, the number ratio of the surface atoms with respect to the total atoms, is very large: 92, 76,

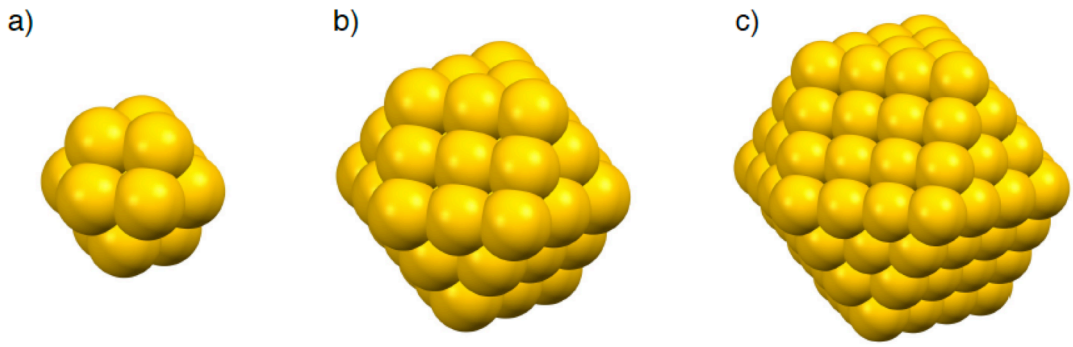

Figure 1.1. Cuboctahedral model structures of metal NSs: M_{13}, M_{55}, and M_{147}.

Table 1.1. Diameter, number and ratio of surface atoms, fraction exposed and coordination number of M_{13}, M_{55}, and M_{147}.

	M_{13}	M_{55}	M_{147}
Diameter (nm)	0.7	1.2	1.7
Number of surface atoms	12	42	92
Fraction exposed (%)	92	76	63
Coordination number	5.5	8.0	9.1

63 % for M_{13}, M_{55}, and M_{147} (M = metal), respectively. Namely, more than half of the constituent atoms of NSs are located on the surface. In addition, there are sites having small coordination numbers that may be reactive toward other molecules. This feature prompted us to apply them for catalysis. As a result of large surface area, the melting temperature is reduced dramatically with the decrease in diameter. For example, the melting point of gold nanospheres (AuNSs) monotonously decreases with the reduction of the diameter (Figure 1.2).[1] The melting temperature (T_m) of a NS with a diameter (d) and molar heat of fusion (L) is estimated by the following Pawlow relation

$$\frac{T_{\mathrm{m}}(\mathrm{r})}{T_{\mathrm{m}}(\infty)} = 1 - \frac{4v_{\mathrm{s}}^{2/3}}{L}\left(\gamma_{\mathrm{s}} 2v_{\mathrm{s}}^{2/3} - \gamma_{\mathrm{l}} 2v_{\mathrm{l}}^{2/3}\right)\frac{1}{d} \tag{1.1}$$

where v, γ_{s}, γ_{l} are the specific molar volume, the surface free energy of the solid, and that of liquid, respectively. $T_m(\infty)$ represent the melting temperature of the bulk metal.

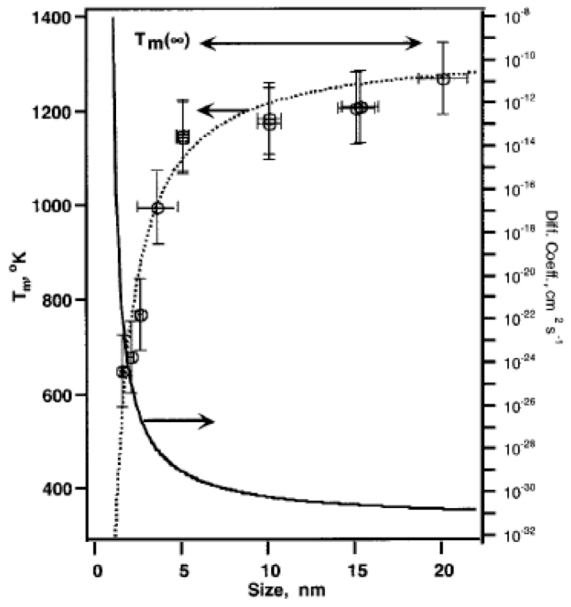

Figure 1.2. Size dependences of the melting point and the diffusion coefficient of AuNSs. The bulk melting temperature of Au is indicated by the double arrow with $T_m(\infty)$.[1] Reprinted from ref. 1 with permission. 2002 American Chemical Society.

As equation 1.1 indicated, the melting temperature is inversely proportional to the particle diameter. In other words, the melting temperature of metal NSs is scalable with respect to *d*. By taking advantage of this feature, metal NSs have been used to make conductive inks and films at low temperature.[2,3]

Metal NSs have long been used as a colorant of stained glass before the understanding of the origin of the vivid colors. Michael Faraday revealed in the mid 1800s that this color was originated from colloidal metal NSs.[4] Later, Gustav Mie explained the origin of the color or the metal NSs in terms of localized surface plasmon resonance (LSPR).[5] LSPRs are collective oscillations of conduction electrons when a metal NSs whose size is smaller than the wavelength of light is irradiated. In response to the oscillating electric field of light, electrons in the metal NSs are displaced from the nuclei of metal. This displacement makes a restoring force due to coulombic attraction between electrons and nuclei.[6] Therefore, this restoring force is strongly depending on the shapes of metal nanostructures (see Sec.1.2.2). The exact solution of the LSPR is given for NSs in 1908. Since the equation based on Mie theory was very complicated, the equation was simplified by assuming the dipole oscillation contributes.[7] The extinction cross-section (C_{ext}) of LSPR is expressed as

$$C_{\mathrm{ext}} = \frac{24\pi^2 R^3 \varepsilon_{\mathrm{m}}^{3/2}}{\lambda} \frac{\varepsilon_2}{(\varepsilon_1 + 2\varepsilon_{\mathrm{m}})^2 + \varepsilon_2^2} \tag{1.2}$$

where *R* is the radius of NS, λ is the wavelength of light, ε_m is the dielectric constant of the surrounding medium, and $\varepsilon = \varepsilon_1 + i\varepsilon_2$ is the complex dielectric constant of the NS. This equation predicts that a resonant peak appears when $\varepsilon_1 = -2\varepsilon_m$ is satisfied.

In case of coinage metal such as Au, Ag, and Cu, the LSPR band appears at ~520, ~360, and ~580 nm, respectively.

1.1.2. Metal clusters

When metal NSs are further miniaturized to ultrafine particles called as clusters, their properties change dramatically. In case of gold, it is known that their structures and properties change drastically at a critical diameter of ~2 nm (Figure 1.3).[8] Recently, it was demonstrated that the atomic structures of thiolate-protected Au clusters undergo a transition from fcc structure to icosahedral or decahedral structures between $Au_{144}(SR)_{60}$ and $Au_{187}(SR)_{68}$. Reduction of the surface energy is a driving force of the transition to non-closest packed structures.

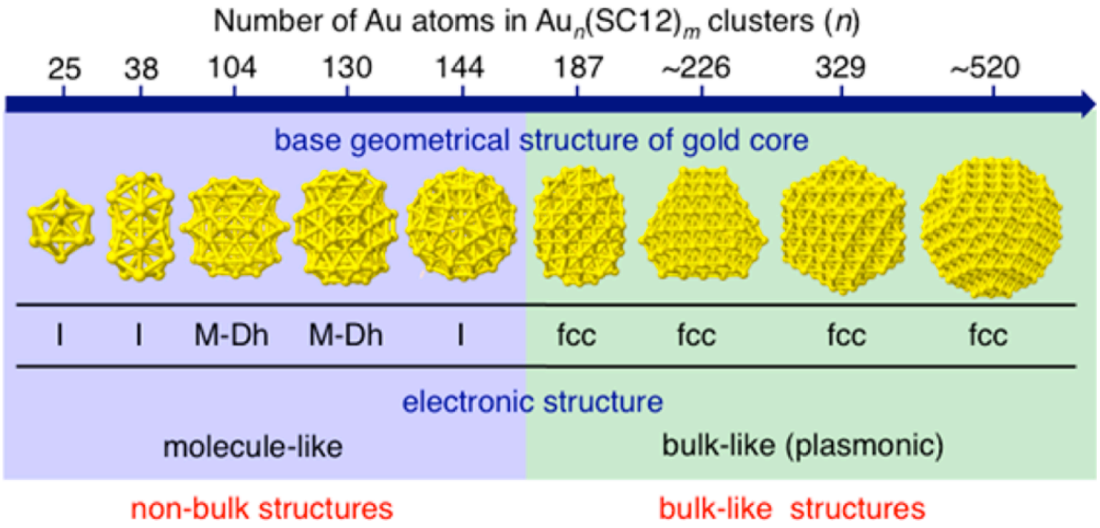

Figure 1.3. Transition of geometric and electronic structures of dodecanethiolate-protected gold clusters.[8] Reprinted from ref. 8 with permission. 2015 American Chemical Society.

The optical response of AuNSs also changes at this size region. As can be seen in Figure 1.4b, the LSPR band reduce the intensity with decrease in the cluster size and disappeared on going from $Au_{187}(SR)_{68}$ to $Au_{144}(SR)_{60}$. The Au clusters smaller than $Au_{144}(SR)_{60}$ exhibit structured optical spectra whose structures become more

pronounced with the decrease in temperature. This optical response of small clusters indicates that single electron transition between quantized levels is induced upon photoirradiation as in the case of conventional molecules. Further reduction of size below $Au_{39}(SR)_{24}$ shows the increase of the HOMO-LUMO gap and appearance of photoluminescence. This is due to the elongation of the lifetime of electronically excited

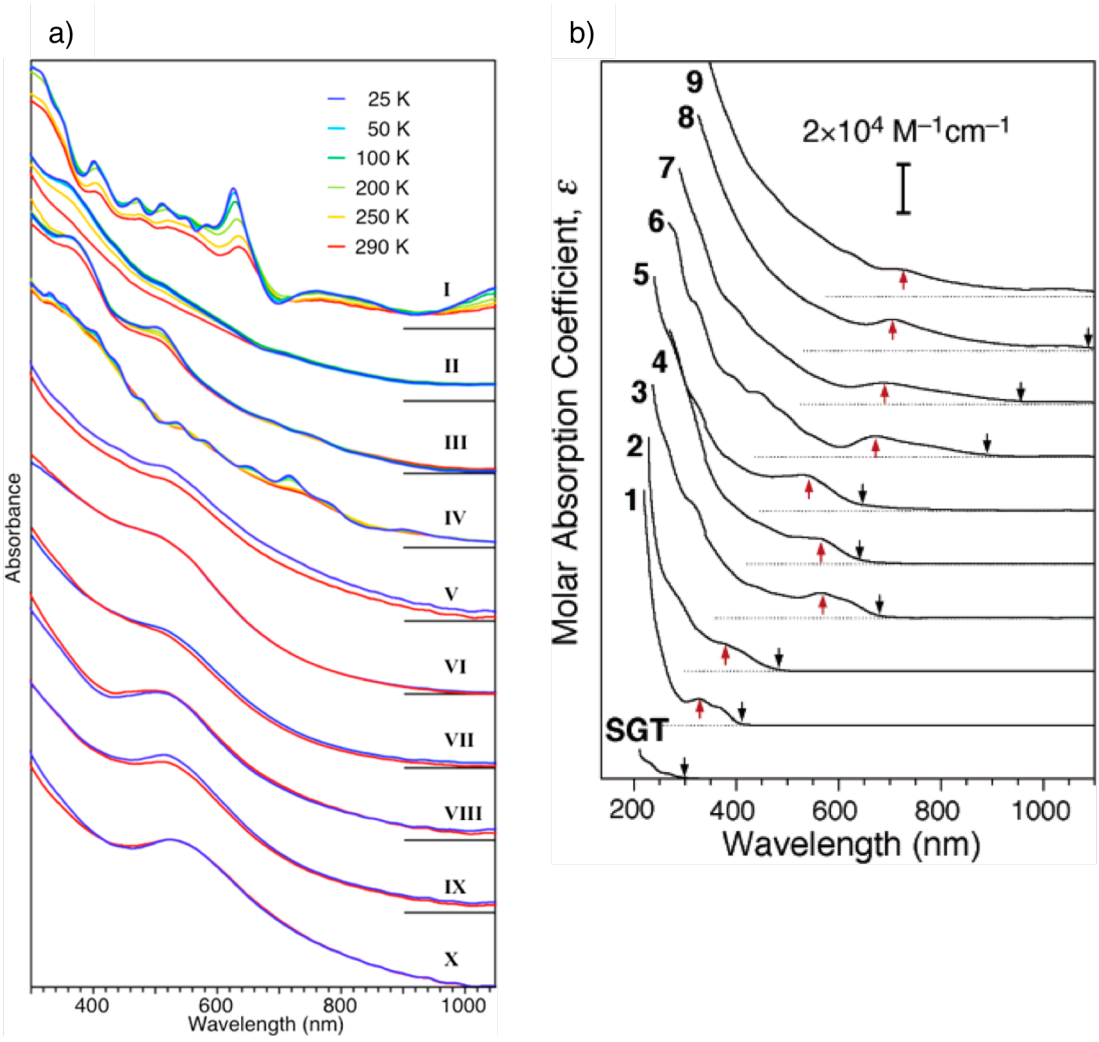

Figure 1.4. Optical spectra of a) dodecanethiolate-protected Au clusters[8] and b) glutathionate-protected Au clusters.[9] I: Au_{38}, II: Au_{104}, III: Au_{130}, IV: Au_{144}, V: Au_{187}, VI: $Au_{\sim 226}$, VII: $Au_{\sim 253}$, VIII: Au_{329}, IX: $Au_{\sim 356}$, X: $Au_{\sim 520}$, 1: Au_{10-12}, , 2: Au_{15}, 3: Au_{18}, 4: Au_{22}, 5: Au_{22}, 6: Au_{25}, 7: Au_{29}, 8: Au_{33}, Au_{35}, 9: Au_{38}, Au_{39} Reprinted from ref. 8, and 1 with permissions for a) and b), respectively. 2015, and 2005 American Chemical Society.

states[10,11] in sharp contrast to the short lifetime of electronically excited states in the bulk due to efficient phonon-electron and electron-electron couplings.[9]

Chemical properties of metal NSs also show non-scalabe behavior in the cluster regime.[12] Typical examples can be found in Au clusters. It is widely known that gold is chemically inert and does not show any catalysis. However, Au clusters exhibit catalytic activities for oxidation reactions. The turn over frequency of oxidation reaction of p-hydroxybenzyl alcohol in Figure 1.5 is enhanced with the decrease of sizes.[13] This size-specific oxidation catalysis of Au clusters has been ascribed to the electronic structure: the key step is proposed to be the activation of oxygen molecule by electron transfer from negatively charged Au clusters.

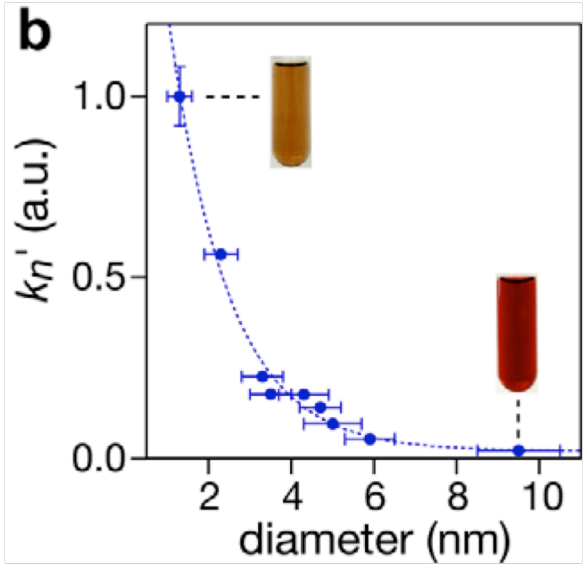

Figure 1.5. Catalytic activity of polymer stabilized Au clusters as a function of the size. Reprinted from ref. 13 with permission. 2006 Elsevier B. V.

As shown above, the metal NSs show interesting properties that are scalable by the diameter. In contrast, metal clusters exhibit novel properties which are not scalable and not predictable with a simple scaling law. This suggests that reduction of the dimension of nanostrucrures below a certain critical dimension (~2 nm in case of gold), we can

expect emergence of unprecedented properties. In this sense, nanoscience can be viewed as a modern alchemy for new materials.

1.2. Anisotropic metal nanostructures

1.2.1. Morphology and properties

Metal nanostructures with various morphologies such as cubes, cages, stars, rods, and wires, exhibit unique properties owing to the unique morphologies have been reported so far. For example, El-Sayed demonstrated that the catalytic properties of Pt and Pd nanostructures depend strongly on their morphology: NSs, nanotriangles, and nanocages.[14] This finding was ascribed to the facet-dependent catalysis. We can regard anisotropy as another parameter to control the properties of metal nanostrucrtures in addition to the diameter.

1.2.2. Gold nanorods

Gold nanorods (AuNRs) have been extensively studied as the representative anisotropic Au nanostructures over the last two decades. One of the breakthroughs in the study of AuNRs is a development of synthetic methods based on template methods.[15,16] In the early stage of the research, AuNRs had been synthesized using a vapor–liquid–solid (VLS) method, which is similar to a chemical vapor deposition used in the synthesis of semiconductor nanowires.[17] In 1997, a new synthesis method has been developed based on electrochemical reduction in hard templates such as porous alumina and polycarbonates.[18] In 2001, the wet chemical synthesis of seed-mediated chemical growth using soft templates of cetyltrimethylammonium bromide (CTAB)[19–21] has been developed (Figure 1.6). TEM studies revealed that AuNRs take fcc structures

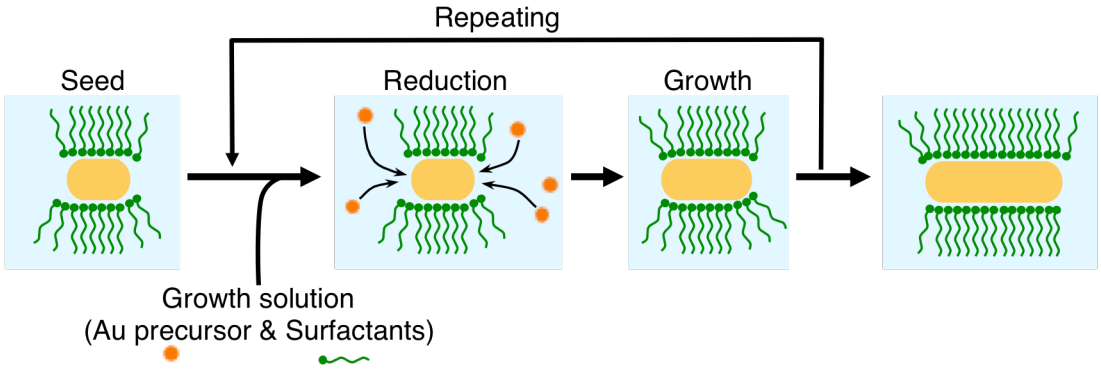

Figure 1.6. Synthetic scheme of seed-mediated growths to form AuNRs.

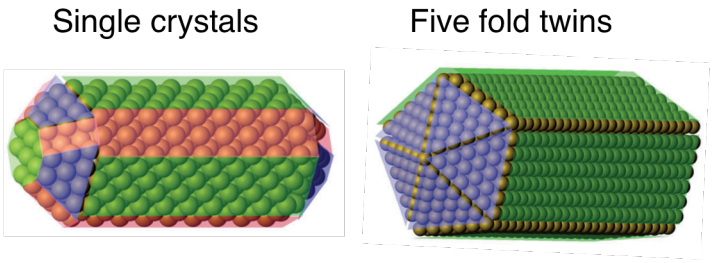

Figure 1.7. Two model structures of AuNRs.[22] Reprinted from ref. 22 with permission. 2011 Royal Society of Chemistry.

of single crystals or five-fold twin structures (Figure 1.7).[22] These crystal structures have been selectively synthesized with or without silver ions.[22] This method of seed-mediated growth enables researchers to synthesize AuNRs with controlled structures reproducibly and promote the studies of various properties of AuNRs.

One of the attractive properties of AuNRs is LSPRs. A correlation between the anisotropic shapes and optical property of LSPRs was theoretically predicted in early 1900s by Gans.[23] The nanostructures with ellipsoid shapes exhibit two modes of LSPRs depending on the orientations of the electric field of light with respect to the ellipsoids. The extinction cross-section (C_{ext}) is given by[7]

$$C_{ext} = \frac{2\pi V \varepsilon_m^{3/2}}{3\lambda} \sum_j \frac{\frac{1}{P_j^2}\varepsilon_2}{(\varepsilon_1 + \frac{1-P_j}{P_j}\varepsilon_m)^2 + \varepsilon_2^2} \tag{1.3}$$

where V is the volume of the rod and P_j (j = a, b, c; $a > b = c$,: a = length, b = c = width) are depolarization factors for ellipsoids. These P_j are expressed as

$$P_{\mathrm{a}} = \frac{1-e^2}{e^2}\left[\frac{1}{2e}\ln\left(\frac{1+e}{1-\mathrm{e}}\right) - 1\right] \tag{1.4}$$

$$P_{\mathrm{b}} = P_{\mathrm{c}} = \frac{1-P_{\mathrm{a}}}{2} \tag{1.5}$$

where e is the rod's ellipticity known as $e^2 = 1 - \xi^{-2}$. ξ is equal to the aspect ratio (length/diameter). As expected from Gans theory, AuNRs exhibited two LSPRs of transverse mode at around 500 nm and longitudinal mode in the Vis–NIR region (Figure 1.8a).[24] These LSPR modes originate from the collective motion of electrons along transverse or longitudinal axes, respectively (Figure 1.8b). A unique feature is that the longitudinal mode of LSPRs can be tunable in the wide range from visible to IR region.[25] The longitudinal mode of LSPRs can be applied to various fields such as photo-catalysis and sensing.[26] Above all, highly tunable longitudinal mode of LSPRs is suitable for applications in the field of biology. By controlling the aspect ratio of AuNRs, the resonant wavelength of LSPRs can be tuned to the optical windows of tissues (650–900 and 1000–1350 nm).[27,28] Excitation of LSPR band of AuNRs with intense laser induces local heating and can be used for plasmonic photothermal therapy. AuNRs irradiated by intense laser are spheroidized and become transparent to the IR light.[29]

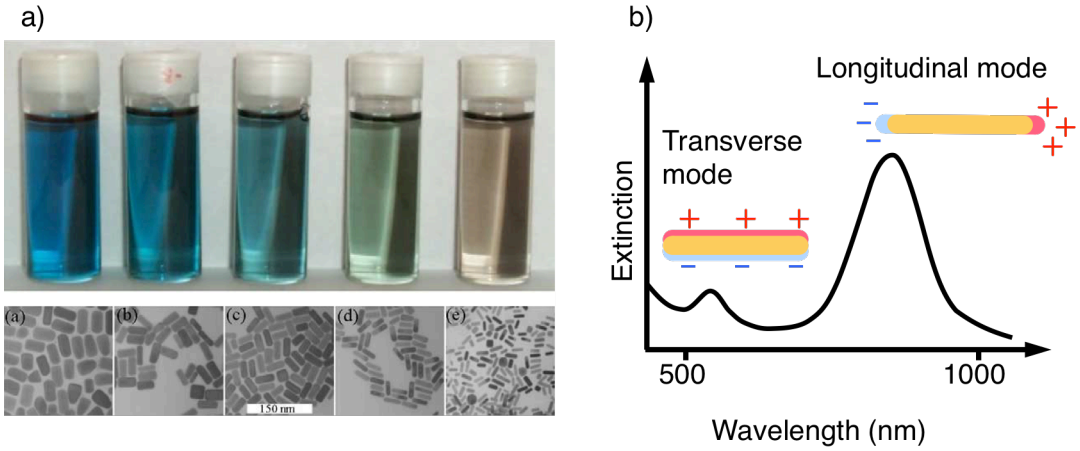

Figure 1.8. a) Dispersions and TEM images of AuNRs.[26] b) Schematic images of optical spectra of AuNRs. Reprinted from ref. 26 with permission for a). 2005 Elsevier B. V.

1.2.3. Ultrathin gold nanorods

Metal NRs are expected to exhibit unique properties when their diameters become smaller than a critical size as observed in isotropic metal NSs. The synthesis of ultrathin gold nanowires (AuUNWs) with a diameter of ~1.6 nm and a length of μm scale has been reported in 2007–2009.[30–34] In these reports, two growth mechanisms have been proposed (Figure 1.9): (1) Oriented attachment of Au clusters and (2) one-dimensional growth of Au(0) atoms. In the former mechanism, small AuNSs formed initially are attached into one-dimensional structures. In the latter mechanism, Au(I) ions arranged one-dimensionally due to aurophilic interaction aggregate into one-dimensional structures upon reduction.

AuUNWs show promise for a variety of applications,[35–43] including mechanical energy storage devices,[37] pressure sensors with fast response, high sensitivity and good stability,[36] flexible electrodes with high transparency and metallic conductivity,[35] bio-sensors using an electrochemical and near-infrared photo-acoustic imaging

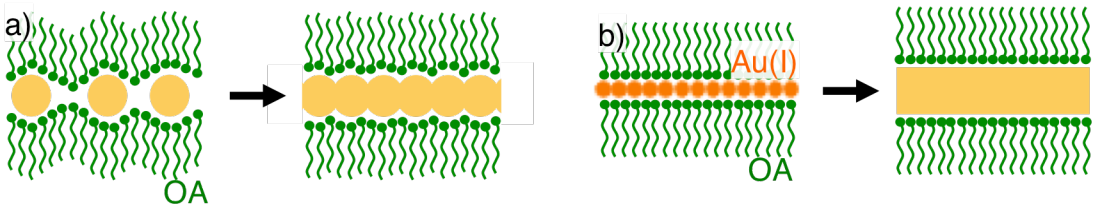

Figure 1.9. Synthesis scheme of AuUNWs: a) oriented attachment and b) one-dimensional chain.

method,[38,39] surface-enhanced Raman scattering (SERS),[34] and catalysis.[40] Thus, the AuUNWs with a diameter of ~1–2 nm are fascinating nanomaterials with new functionalities.

Smaller, atomically-precise anisotropic Au clusters have already been reported since 2007. For example, single crystal X-ray diffraction (SXRD) analysis of $[Au_{25}(PPh_3)_{10}(SC_{12}H_{25})_5Cl_2]^{2+}$ (ref. 44, Figure 1.10a) and $Au_{38}(SC_2H_4Ph)_{18}$ (ref. 45, Figure 1.10b) revealed that these two clusters are constructed by two icosahedral Au_{13} clusters bonded via vertex-shared and facet-shared bonding, respectively. Very recently, anisotropic Au clusters with an aspect ratios larger than ~3 have been reported. $[Au_{37}(PPh_3)_{10}(SC_2H_4Ph)_{10}Cl_2]^{+}$ (ref. 46, Figure 1.10c) has a tri-icosahedral core which shares a vertex Au atoms with three Au_{13} icosahedrons. Another series of anisotropic Au clusters which are composed of cuboctahedral Au_{13} have been also reported. Two anisotropic Au clusters of $Au_{28}(TBBT)_{20}$ (ref. 47) and $Au_{30}S(S\textit{t}Bu)_{18}$ (ref. 48) consist of two interpenetrating Au_{13} cuboctahedrons. $Au_{76}(4\text{-MEBA})_{44}$ (ref. 49, Figure 1.10d) composed of five face-sharing Au_{13} cuboctahedra was also reported. These clusters exhibit intense peaks in IR region (Figure 1.11) that are not assigned to LSPR but to a single electron transition between molecular-like discrete electronic levels. On the other hand, theoretical simulation suggests that one-dimensional polymers of Au_{13}

icosahedrons exhibit the different electrical conductivity depending on the vertex-shared or facet-shared bonding.[50]

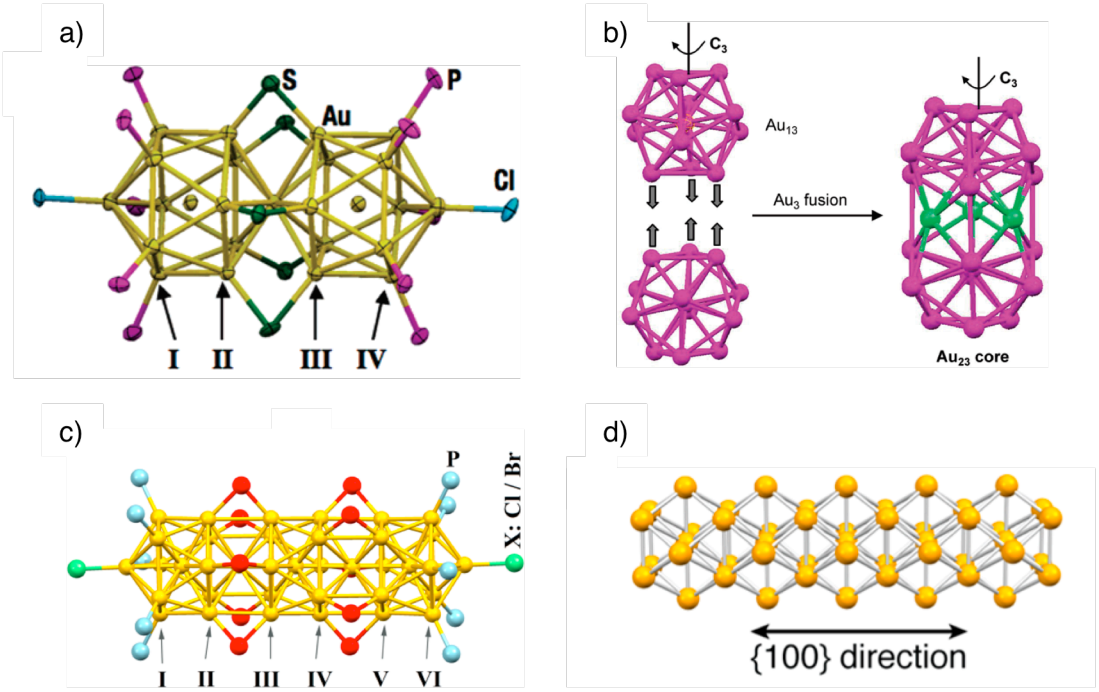

Figure 1.10. Atomic structures of a) Au_{25} (ref. 44), b) Au_{24} (ref. 45), c) Au_{37} (ref. 46), and d) Au_{49} (ref. 49) cores in clusters. Reprinted from ref. 44, 45, 46, and 49 with permissions. 2007, 2010, 2015, and 2015 American Chemical Society.

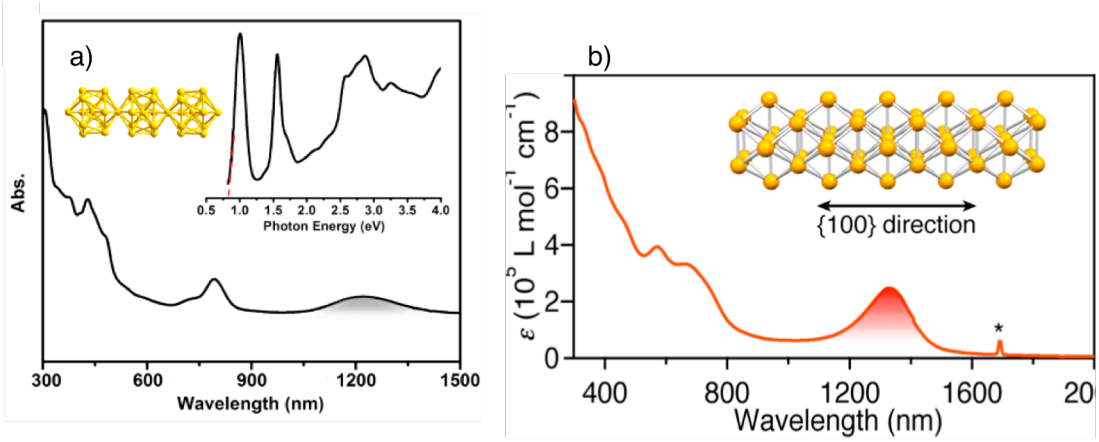

Figure 1.11. UV–vis–NIR spectra of a) Au_{37} (ref. 46) and b) Au_{49} (ref. 49) cores in clusters. The peaks in NIR region are highlighted by gray and red for Au_{37}, and Au_{49} respectively. Reprinted from ref. 46, and ref. 49 with permissions. 2015 American Chemical Society.

1.3. Aim of this study

1.3.1. Target and aim

The target nanostructure of this thesis is ultrathin Au nanorods (AuUNRs, Figure 1.12). The diameter of AuUNRs is much thinner than those of conventional AuNRs (>10 nm), but comparable to ~2 nm at which remarkable transitions of electronic and geometric structures take place (Figure 1.3). However, less is known about the structures and properties AuUNRs mainly because their synthetic method has not been developed since the first report in 2008.[51] Therefore, the following questions arise concerning the structures and properties of AuUNRs: (1) Do the AuUNRs have single crystals or twinned crystal structures? (2) Do the AuUNRs exhibit LSPRs? If yes, is the

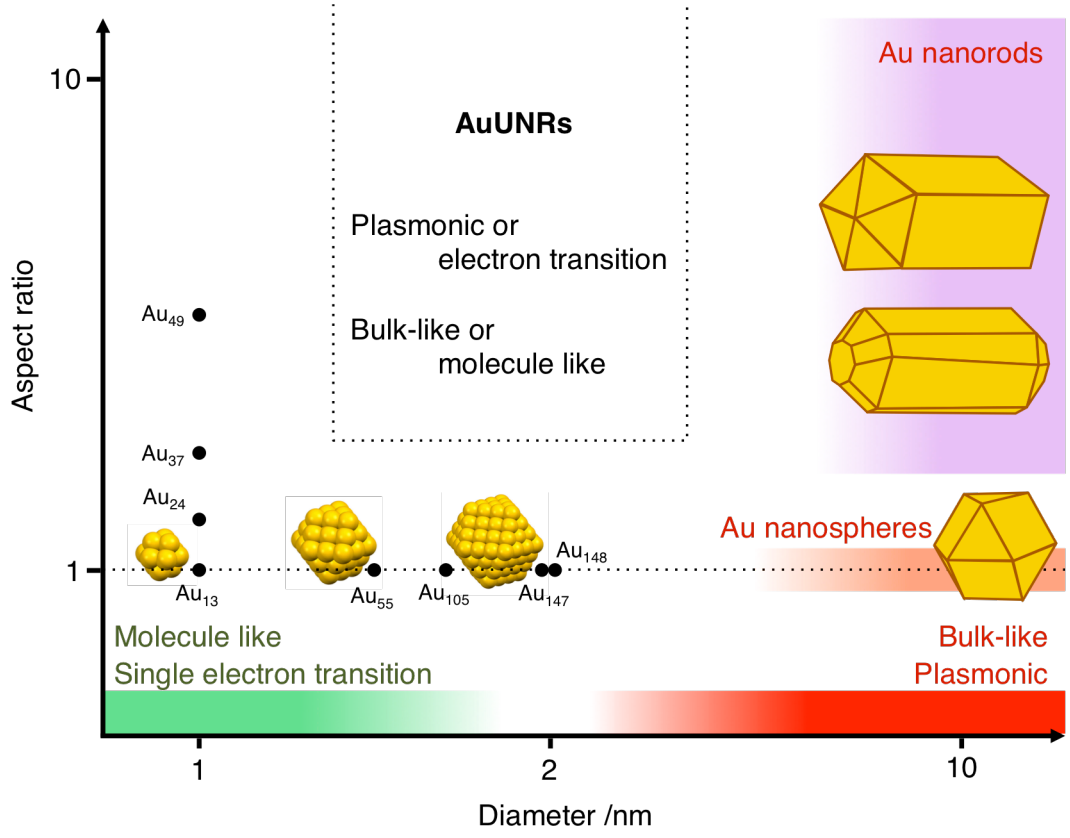

Figure 1.12. Target of this study.

correlation between wavelength and aspect ratio similar to that of the conventional AuNRs? (3) What determines the morphology of the AuUNRs?

1.3.2. Challenges

To answer these questions, there are several challenges that must be overcome. The first challenge is the synthesis of AuUNRs with well-defined size control and chemical modification of the surface. In case of synthesis of AuNRs, the length of AuNRs has been controlled by chain length of surfactants and concentration of silver ions.[16] On the other hand, as for AuUNWs, it is not clear what the factor controls the length of AuUNRs.

The second challenge is the determination of atomic structures of AuUNRs. Transmission electron microscopy is a powerful tool to observe the morphology and atomic structures of small particles that cannot be crystalized. The spatial resolution δ is estimated by $\delta = \sim\lambda$. where λ is the wavelength of radiation. The resolution of TEM is given by

$$\lambda\,(\mathrm{nm}) = \frac{1.22}{E^{1/2}} \tag{1.6}$$

where E is electron energy in electron volts.[52] For a 100 keV TEM, λ is calculated to be ~4 pm, which is sufficient to observe the atomic structures of Au nanostructures theoretically. However, the spatial resolution of TEM is limited mainly due to chromatic and spherical aberrations. The chromatic aberration originates from the dispersion of the kinetic energy of electrons: the electrons with different kinetic energies focus at different points. The contribution from chromatic aberration is negligibly small if the TEM samples are thin enough. On the other hand, the spherical

aberration leads to lowering the resolutions of TEM. The electrons focus at different points depending on their electron paths because the electromagnetic lenses in TEM are not perfect and the error of focuses becomes large especially in off-center electron paths in the lenses. This spherical aberration is corrected using extra electromagnetic lens and as a result, the resolution up to ~1Å is improved. In this thesis, the samples of AuUNRs are so thin that the chromatic aberration is the negligible. Therefore, TEM that is equipped with the spherical aberration corrector (aberration corrected TEM: AC TEM) was used for observation of atomic structures.

1.3.3. Outline

The present thesis is organized as follows.

In Chapter 2, I report the length control method of AuUNWs and AuUNRs by reducing the concentrations of reagents and the surface modification methods by thiolates.

In Chapter 3, I report optical properties of AuUNRs. I correlate the resonant wavelengths with aspect ratio. The correlation of AuUNRs are compared with that of conventional AuNRs with diameters of >10 nm. I revealed that resonant wavelength of LSPRs of AuUNRs is remarkably red shifted, compared to that of AuNRs with same aspect ratios.

In Chapter 4, I observe crystal structures by using AC HRTEM, and analyze these TEM images statistically, and propose the model atomic structures. The formation process of atomic structures of AuUNRs is investigated.

In Chapter 5, I reveal the decomposition mechanisms of AuUNRs in dispersions without excess amount of OA and surfactant-concentration and temperature dependence

on stability of AuUNRs. I also report the improvement of stability of AuUNRs via the surface modification from amines to thiolates.

In Chapter 6, I describe the concluding remarks including summary of the contents and future prospects.

References

1. Dick, K.; Dhanasekaran, T.; Zhang, Z.; Meisel, D. *J. Am. Chem. Soc.* **2002**, *124*, 2312–2317.
2. Kamyshny, A.; Magdassi, S. *Small* **2014**, *10*, 3515–3535.
3. Kim, D.; Moon, J. *Electrochem. Solid State* **2005**, *8*, J30–J33.
4. Faraday, M. *Phil. Trans. R. Soc. Lond.* **1857**, *147*, 145–181.
5. Mie, G. *Ann. Phys.* **1908**, *25*, 377–445.
6. Kelly, K. L.; Cornado, E.; Zhao, L. L.; Schatz, G. C. *J. Phys. Chem. B* **2003**, *107*, 668–677.
7. Hu, M.; Chen, J.; Li, Z.-Y.; Au, L.; Hartland, G. V.; Li, X.; Marquez, M.; Xia, Y. *Chem. Soc. Rev.* **2006**, *35*, 1084−1094.
8. Negishi, Y.; Nakazaki, T.; Malola, S.; Takano, S.; Niihori, Y.; Kurashige, W.; Yamazoe, S.; Tsukuda, T.; Häkkinen, H. *J. Am. Chem. Soc.* **2015**, *137*, 1206–1212.
9. Negishi, Y.; Nobusada, K.; Tsukuda, T. *J. Am. Chem. Soc.* **2005**, *127*, 5261–5270.
10. Wilcoxon, J. P.; Martin, J. E.; Parsapour, F.; Wiedenman, B.; Kelley, D. F. *J. Chem. Phys.* **1998**, *108*, 9137–9143.
11. Huang, T.; Murray, R. W. *J. Phys. Chem. B* **2001**, *105*, 12498–12502.
12. Yamazoe, S.; Koyasu, K.; Tsukuda, T. *Acc. Chem. Res.* **2014**, *47*, 816–824.
13. Tsunoyama, H.; Sakurai, H.; Tsukuda, T. *Chem. Phys. Lett.* **2009**, *429*, 528–532.
14. Mahmoud, M. A.; Narayanan, R.; El-Sayed, M. A. *Acc. Chem. Res.* **2013**, *46*, 1795–1805.
15. Lohse, S. E.; Murphy, C. J. *Chem Mater.* **2013**, *125*, 1250–1261.
16. Huang, X.; Neretina, S.; El-Sayed, M. A. *Adv. Mater.* **2009**, *21*, 4880–4910.
17. Dick, K. A. *Prog. Cryst. Grow. Charac. Mater.* **2008**, *54*, 138–173.
18. Yu, Y.; Chang, S. S.; Lee, C. L.; Wang, C. R. *J. Phys.. Chem. B* **1997**, *101*, 6661–6664.
19. Yu, Y.-Y.; Chang, S.-S.; Lee, C.-L.; Wang, C. R. C. *J. Phys. Chem. B* **1997**, *101*, 6661–6664.
20. Jana, N. R.; Gearheart, L.; Murphy, C. J. *J. Phys. Chem. B* **2001**, *105*, 4065–4067.
21. Nikoobakht, B.; El-Sayed, M. A. *Chem. Mater.* **2003**, *15*, 1957–1962.
22. Liu, K.; Zhao, N.; Kumacheva, E. *Chem. Soc. Rev.* **2011**, *40*, 656–671.
23. Gans, R.; Ann. Phys. **1915**, *47*, 270–284.
24. Jain, P.; Huang, X.; El-Sayed, I. H.; El-Sayed, M. A. *Acc. Chem. Res.* **2008**, *41*, 1578–1586.
25. Hu, M.; Chen, J.; Li, Z.-Y.; Au, L.; Hartlandm, G. V.; Li, X.; Marquez, M.; Xia, Y. *Chem. Soc. Rev.* **2006**, *35*, 1084–1094.
26. Pérez-Juste, J.; Pastoriza-Santos, I.; Liz-Marzán, L. M.; Mulvaney, P. *Coord. Chem. Rev.* **2005**, *249*, 1870–1901.

27. Weissleder, R. A. *Nat. Biotechnol.* **2001**, *19*, 316–317.
28. Smith, A. M.; Mancini, M. C.; Nie, S. **2009**, *Nat. Nanotechnol.* **2009**, *4*, 710–711.
29. Qin, Y.; Liu, L.; Yang, R.; Gösele, U.; Knez, M. *Nano Lett.* **2008,** *8*, 3221–3225.
30. Halder, A.; Ravishankar, N. *Adv. Mater.* **2007**, *19*, 1854–1858.
31. Huo, Z.; Tsung, C.-k.; Huang, W.; Zhang, X.; Yang, P. *Nano, Lett.* **2008**, *8*, 2041–2044.
32. Pazos-Pérez, N.; Baranov, D.; Irsen, S.; Hilgendorff, m.; Liz-Marzán, L. M.; Giersig, M. *Langmuir* **2008**, *24*, 9855–9860.
33. Lu, X.; Yavuz, M. S.; Tuan, H.-Y.; Korgel, B. A.; Xia, Y. *J. Am. Chem. Soc.* **2008**, *130*, 8900–8901.
34. Feng, H.; Yang, Y.; You, Y.; Li, G.; Guo, J.; Yu, T.; Shen, Z.; Wu, T.; Xing, B. *Chem. Commun.* **2009**, 1984–1986.
35. Xu, J.; Wang, H.; Liu, C.; Yang, Y.; Chen, T.; Wang, Y.; Wang, F.; Liu, X.; Xing, B.; Chen, H. *J. Am. Chem. Soc.* **2010**, *132*, 11920.
36. Gong, S.; Schwalb, W.; Wang, Y.; Chen, Y.; Tang, Y.; Si, J.; Shirinzadeh, B.; Cheng, W. *Nat. Commun*. **2014**, *5*, 3132.
37. Azulai, D.; Belenkova, T.; Gilon, H.; Barkay, Z.; Markovich, G. *Nano Lett.* **2009**, *9*, 4246–4249.
38. Cui, H.; Hong, C.; Ying, A.; Yang, X.; Ren, S. *ACS Nano* **2013**, *7*, 7805–7811.
39. Koposova, E.; Kisner, A.; Shumilova, G.; Ermolenko, Y.; Offenhäusser, A.; Mourzina, Y. *J. Phys. Chem. C* **2013**, *117*, 13944–13951.
40. Hu, L.; Cao, X.; Yang, J.; Li, M.; Hong, H.; Xu, Q.; Ge, J.; Wang, L.; Lu, J.; Chen, L.; Gu, H. *Chem. Commun.* **2011**, *47*, 1303.
41. Pud, S.; Kisner, A.; Heggen, M.; Belaineh, D.; Temirov, R.; Simon, U.; Offenhäusser, A.; Mourzina, Y.; Vitusevich, S. *Small* **2013**, *9*, 846.
42. Chandri, U.; Kundu, P.; Singh, A. K.; Ravishankar, N.; Ghosh, A. *ACS Nano* **2011**, *5*, 8398–8403.
43. Chandri, U.; Kundu, P.; Kundu, S.; Ravishankar, N.; Ghosh, A. *Adv. Mater.* **2013**, *25*, 2486–2491.
44. Shichibu, Y.; Negishi, Y.; Watanabe, T.; Chaki, N. K.; Kawaguchi, H.; Tsukuda, T. *J. Phys. Chem. C* **2007**, *111*, 7845–7847.
45. Qian, H.; Echenhoff, W.; Zhu, Y.; Pintauer, T.; Jin, R. *J. Am. Chem. Soc.* **2010**, *132*, 8280–8281.
46. Jin, R.; Liu, C.; Zhao, S.; Das, A.; Xing, H.; Gayathri, C.; Xing, Y.; Rosi, N. L.; Gil, R. R. Jin, R. *ACS Nano*, **2015**, *9*, 8530–8536.
47. Zeng, C.; Li, T.; Das, A.; Rosi, N. L.; Jin, R. *J. Am. Chem. Soc.* **2013**, *135*, 10011–10013.
48. Yang, H.; Wang, Y.; Edwards, A. J.; Yan, J.; Zheng, N. *Chem. Commun.* **2014**, *50*, 14325–

14327.

49. Takano, S.; Yamazoe, S.; Koyasu, K.; Tsukuda, T. *J. Am. Chem. Soc.* **2015**, *137*, 7027–7030.
50. Jiang, D.-e.; Nobusada, K.; Luo, W.; Whetten, R. L. *ACS Nano* **2009**, *3*, 2351–2357.
51. Li, Z.; Tao, J.; Lu, X.; Zhu, Y.; Xia, Y. *Nano Lett.* **2008**, *8*, 3052–3055.
52. *Transmission Electron Microscopy*, Williams, D. B., Carter, C. B., Eds,; Springer, 2009.

Chapter 2.

Length controlled synthesis and surface modification

A part of this chapter has been published in a following paper.
Ryo Takahata, Seiji Yamazoe, Kiichirou Koyasu, Tatsuya Tsukuda
J. Am. Chem. Soc. **2014**, *136*, 8489–8491.

本章については、5 年以内に雑誌等で刊行予定のため、非公開。

Chapter 3.

Optical properties: localized surface plasmon resonance

A part of this chapter has been published in a following paper.
Ryo Takahata, Seiji Yamazoe, Kiichirou Koyasu, Tatsuya Tsukuda,
J. Am. Chem. Soc. **2014**, *136*, 8489–8491.

本章については、5 年以内に雑誌等で刊行予定のため、非公開。

Chapter 4.

Atomic structures and model structure

A major part of this chapter has been published in a following paper.

Ryo Takahata, Seiji Yamazoe, Kiichirou Koyasu, Tatsuya Tsukuda,

J. Phys. Chem. C **2017**, *121*, 10942–10947.

本章については、5 年以内に雑誌等で刊行予定のため、非公開。

Chapter 5.

Morphological stability

A major part of this chapter has been published in a following paper.

Ryo Takahata, Seiji Yamazoe, Chompunuch Warakulwit, Jumras Limtrakul, Tatsuya Tsukuda,

J. Phys. Chem. C **2016**, *120*, 17006–17010.

本章については、5 年以内に雑誌等で刊行予定のため、非公開。

Chapter 6.

Concluding remarks

本章については、5 年以内に雑誌等で刊行予定のため、非公開。

List of Publications

Publications related to the thesis

1. "Structural Model of Ultrathin Gold Nanorods Based on High-Resolution Transmission Electron Microscopy: Twinned 1D Oligomers of Cuboctahedrons", Ryo Takahata, Seiji Yamazoe, Kiichirou Koyasu, Tatsuya Tsukuda, *J. Phys. Chem. C* **2017**, *121*, 10942–10947.

2. "Rayleigh Instability and Surface-Mediated Stabilization of Ultrathin Gold Nanorods", Ryo Takahata, Seiji Yamazoe, Chompunuch Warakulwit, Jumras Limtrakul, Tatsuya Tsukuda, *J. Phys. Chem. C* **2016**, *120*, 17006–17010.

3. "Surface Plasmon Resonance in Gold Ultrathin Nanorods and Nanowires", Ryo Takahata, Seiji Yamazoe, Kiichirou Koyasu, Tatsuya Tsukuda, *J. Am. Chem. Soc.* **2014**, *136*, 8489–8491.

Publications not related to the thesis

1. "Monodisperse Iridium Clusters Protected by Phenyl Acetylene: Implication for Size-Dependent Evolution of Binding Sites", Hiroki Yamamoto, Prasenjit Maity, Ryo Takahata, Seiji Yamazoe, Kiichirou Koyasu, Wataru Kurashige, Yuichi Negishi, Tatsuya Tsukuda, *J. Phys. Chem. C* **2016**, *121*, 10942–10947.

2. "Synthesis and Catalytic Application of Ag_{44} Clusters Supported on Mesoporous Carbon", Masaru Urushizaki, Hirokazu Kitazawa, Shinjiro Takano, Ryo Takahata, Seiji Yamazoe, Tatsuya Tsukuda, *J. Phys. Chem. C* **2015**, *119*, 27483–27488.

3. "Thiolate-Mediated Selectivity Control in Aerobic Alcohol Oxidation by Porous Carbon-Supported Au_{25} Clusters", Tatchamapan Yoskamtorn, Seiji Yamazoe, Ryo Takahata, Jun-ichi Nishigaki, Anawat Thivasasith, Jumras Limtrakul, Tatsuya Tsukuda, *ACS Catal.* **2014**, *4*, 3696–3700.

Acknowledgements

I would like to express the deepest appreciation to Prof. Tatsuya Tsukuda. He always gave me an adequate research environment and many suggestions with insightful views for all of this thesis work. Without his committed supports, I could not achieve this work. Also, his sophisticated and earnest working style gives me definite criteria for top scientist.

Discussions about my work with Associate Prof. Kiichirou Koyasu have been fruitful. He always gave me various important suggestions from the theoretical aspects and many prominent skills for vacuum experiments. Associate Prof. Seiji Yamazoe constantly gave the comments with rich ideas based on the material science. My experimental skills mainly learned from his excellent experimental techniques.

I would like to appreciate Prof. Hiroshi Nishihara and Prof. Eiichi Nakamura in the univ. of Tokyo for providing me to access to the TEM apparatus. I would like to thank Prof. Toshiharu Teranishi in Kyoto univ., and Prof. Kohei Imura in Waseda univ. for fruitful discussions of LSPRs.

I wish to thank to Dr. Kiyofumi Nitta (JASRI) for his kind experimental supports and advises. I am thankful to Associate Prof. Dr. Jun-ichi Nishigaki (Tokyo Metropolitan Univ.) for giving me useful advises of wet synthesis. I thank Mr. Koshi Chiba for management of TEM.

I deeply thank to Ms. Yuka Sakurai for wide-range supports in daily life. I also thank Mr. Satoru Muramatsu for discussion of various topics. I am grateful to current group members, Dr. S. Takano Mr. S. Hayashi, Mr. R. Tomihara, Mr. K. Hirata, Mr. S. Emori, Mr. K. Tsuruoka, Mr. H. Yamada, Mr. H. Yamamoto, Mr. T. Omoda, Mr. N. Sasaki, Mr. D. Shuto, Mr. T. Yanase, Mr. N. Shinjo, Mr. Y. Nakajima, Mr. S. Hasegawa, Mr. R. Horie, Mr. K. Kuenhee, Mr. W. L. Lim, Mr. H. Yamazaki, Mr. H. Hirai, Mr. A. Matsuo, and Mr. M. Shimojima for their kind attitudes. I am also grateful to the former members, Dr. H. Kitazawa, Dr. T. Watanabe, Dr. M. J. Sharif, Dr. J. Sharif, Dr. M. J. Jakir, Dr. P. Maity, Mr A. Yanagimachi, Mr. M. Urushizaki, Ms. S. Arii, Mr. S. Matsuo Mr. Y. Kawahara, Ms. T. Yoskamtorn, Mr. D. J. Guzman, Mr. S., Matsuo, Mr. T. Misumi, Mr. R. Ishida, Mr. T. Higaki, Mr. R. Shibuya, and Mr. K. Yamashita.

I wish to thank to a JSPS Research Fellowship for Young Scientists and a SPring-8 Budding Researchers Support (JASRI) for funding.

Finally, I express my sincerest gratitude to my family for their ceaseless affection and support.

Ryo Takahata

January 2018